Sacrificial membranes for serial valving in microsystems

M. Allain*, J. Berthier*, S. Basrour**, and P. Pouteau*

*CEA-LETI, Department of Technology for Biology and Health
17, avenue des Martyrs, 38054 Grenoble, France
** TIMA-MNS, Université Joseph Fourier, Grenoble
marjolaine.allain@cea.fr; jean.berthier@cea.fr

ABSTRACT

Valving is essential to microflow circuits in microsystem technology. Many different types of valves have already been designed. Membranes of sacrificial material have already been studied for one shot valving; however, the new design proposed here, based on sacrificial micro-membranes with embedded electrodes, has the advantages to be efficient, easy to pilot and can connect easily one by one a series of initially isolated micro-chambers implemented in a silicon chip.

Keywords: sacrificial membrane, valve, electrodes, Joule effect, dilatation

1 INTRODUCTION

In the recent years, fluidic microsytems have gained in complexity in order to integrate more and more potentialities; valving has become essential for today fluidic microsystems. Many types of valves exist using different physical principles as capillarity [1], air traps, melts [2], piezo-electric membranes [3], flexible membrane deformation [4], magnetic plugs [5], etc. Micro-valves can be passive or active, one shot or reversible [6]. Valves often carry challenges such as complex fabrication and packaging, moving parts, bulky external actuation principles, leakage, and discrimination towards liquids commonly used in biotechnology.

Sacrificial Si_3N_4 membranes have been studied as one shot valves [7]. In this work we present a new type of such valves with incorporated electrodes (fig. 1). The principle is simple and efficient, but requires precise dimensioning. In the initial state, the different microfluidic domains of the microsystem are separated by thin membranes that resist to a pressure up to 1 bar. A loop electrode made of gold or platinum is inserted in a grooved channel etched in the membrane. Upon electric actuation at a relatively low potential, in a very short time, Joule-heating thermal dilatation of the electrode develops a considerable stress resulting in the breakup of the membrane.

In this paper, we first present the concept and the microfabrication of the membrane, next we show how the membrane has been dimensioned by a numerical approach consisting in coupling a mechanical resistance calculation to a thermal and electrical calculation. Finally, we present the preliminary experiments that have been performed in order to determine the breakup stress.

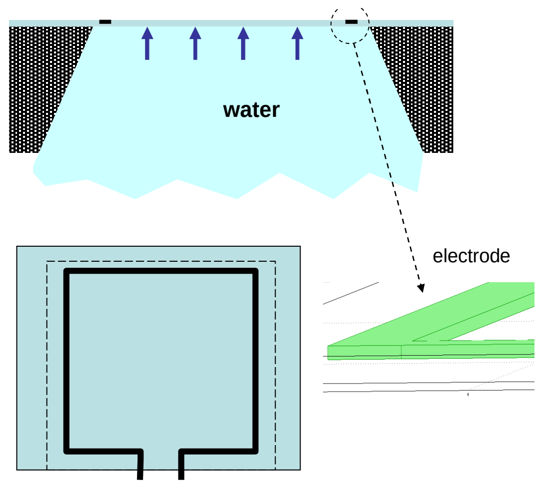

Fig.1. Schematic view of the membrane with the electrodes: The water on the downside facet exerts an upward pressure (top); the electrode follows the edge of the membrane (bottom).

2 CONCEPT AND MICROFABRICATION

The originality of the device is constituted by the electrodes which are incorporated into the membrane, allowing maximization of the mechanical stress. In particular, the tearing off of the electrode from the nitride membrane—that could occur if the electrode was just deposited on the membrane surface—is avoided [7]. However this geometry infers microfabrication constraints because the electrode must necessarily fill and adhere to the grooves etched into the silicon nitride. Microfabrication process begins with a LPCVD silicon nitride deposition. This material has been selected for its good mechanical properties. A groove is then etched in the silicon nitride and the electrode deposited with a lift off technique. Next, the membrane is released by the silicon deep etching (DRIE) processed in the back face (figure 2). Membrane thickness corresponds to that of the deposed nitride layer, e.g. 200nm. With the LPCVD deposition process, the residual stress in the layer (about 500MPa) is tensile, and the membrane is flat.

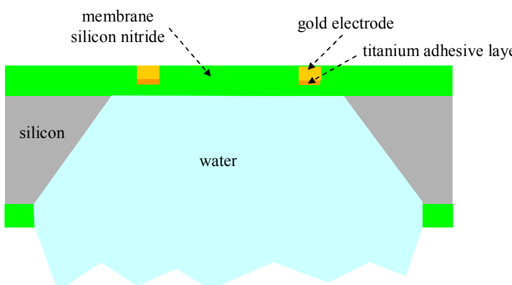

Fig. 2 Detail of the membrane materials.

3 ELECTROTHERMAL CALCULATION

In this section, we present the fast transient Joule-heating of the membrane.

3.1 Transient heat source

The electric field is solution of the electric equation

$$\nabla.(-\sigma \nabla V) = 0 \tag{1}$$

Due to thermal considerations which will be justified later on, the source term is an applied voltage assigned between the two boundaries of the electrode during a brief time interval. Mathematically, the voltage is given by the smoothed Heaviside function superposition

$$V = V_0 \left[H(t,t_0) - H(t,t_1) \right] \tag{2}$$

where V_0 =3 V and t_1-t_0 =10^{-4} s. The electric current circulating in the electrode is

$$j = -\sigma \nabla V \tag{3}$$

Due to the conductivity contrast, the electric current is restricted to the electrode as shown in figure 3. Joule heating is the source term for the thermal problem, which general form is

$$\rho C_p \frac{\partial T}{\partial t} = \nabla.(k \nabla T) + \sigma (\nabla V)^2 \tag{4}$$

Boundary conditions are required to solve for (4). These thermal boundary conditions are complicated because the geometrical domain where temperature diffuses can not be accurately modeled due computational memory limitation. Heat transfer by radiation through the air above the membrane, by conduction in the water below and to the surrounding silicon must be specified. Radiative heat transfer from the upper surface is determined by a radiative heat condition

$$\varphi = \sigma_R \left(T^4 - T_0^4 \right) \tag{5}$$

where $\sigma_R \approx 5.8\ 10^{-8}$ W/m^2/K^4 is the Stefan-Boltzman constant. On the other hand, taking into account a transient diffusion length, the heat transfer by conduction can be written as

$$\varphi = h\left(T - T_0\right) \approx \frac{k}{\delta}\left(T - T_0\right) \approx \frac{1}{2}\sqrt{\frac{k \rho C_p}{t}}\left(T - T_0\right) \tag{6}$$

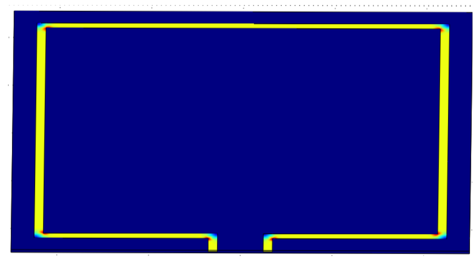

Fig.3. Electric current is restricted to the electrode, with some corners effects.

Solution of (4) with the boundary conditions (5) and (6), together with the Joule heating term deduced from (3) shows that the membrane is submitted to a very brief, but intense temperature pulse (fig. 4.a). Figure 4.b shows the distribution of temperature in the membrane. Even for this fast transient, temperature diffuses somewhat into the membrane. It is important that the heat diffusion in the membrane is not too important, because it would reduce the stress exerted by the dilatation of the electrode. Hence, the heating transient must be very fast.

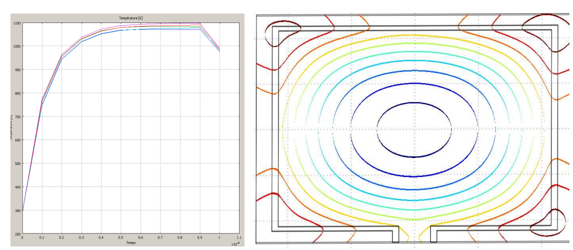

Fig.4. (a) Temperature transient calculated at different locations in the electrode; (b) contour plot for temperatures: the electrode is the hottest part, especially in the corners where the temperature can reach 1000 K for less than 2.10^{-5} seconds. The temperature in the middle stays below 600 K.

3.2 Material properties and non linearity

As the temperature can be high very locally (in less than a few μ^3) the variation of the electric conductivity of gold with temperature must be taken into account. The electric conductivity of gold can be deduced from its thermal conductivity using the Wiedemann-Franz law. The thermal conductivity of gold can be approximated by the relation

NSTI-Nanotech 2009, www.nsti.org, ISBN 978-1-4398-1784-1 Vol. 3, 2009

$$k = k_0 \left[1 - 5.64\ 10^{-4}\ (T - 300)\right] \quad (7)$$

Using the Wiedemann-Franz law for gold, we find the relation between electric and thermal conductivity

$$\sigma = k/L\,T \quad (8)$$

where L is the Lorenz constant (L=2.35 10^{-8} W Ω/K^2). Then

$$\sigma = k_0 \left[1 - 5.64\ 10^{-4}\ (T - 300)\right] / LT \quad (9)$$

The variation of the electric conductivity with the temperature is far from negligible (fig. 5) and necessitates the coupling of the two electrical and thermal equations (1) and (4). Moreover, the variation of k and σ with the temperature renders equation (4) non linear.

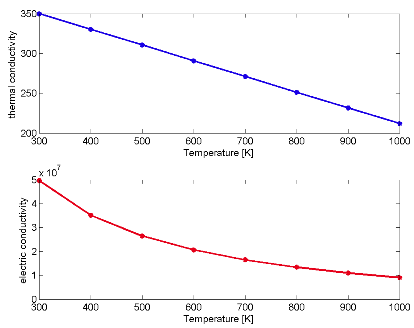

Fig.5. Variation of k and σ with temperature.

3.3. Nano-bubbles and nano-boiling

Another of the reasons to use a very short power transient is to avoid bulk boiling of the water in the microsystem. However, it is likely that the large heat flux during the power pulse—even if its duration is less than 0.1 ms—induces some boiling of the water at the contact with the membrane. Nucleation of nanobubbles is still a subject of research. But it has been shown that very fast pulses can produce nanobubbles [8,9]. This nucleation has two consequences: cavitation may occur after the power pulse, when the bubbles collapse, and may trigger a pressure wave in the system. However, this pressure wave is expected to be damped by the opening of the valve. Another effect of nucleation is the change in the heat transfer to the liquid. It is well established that, for macroscopic and microscopic geometries as well, nucleate boiling enhances heat transfer [10]. As for now, we will keep equation (6) and check its validity against experiments.

4 MECHANICAL CALCULATION

At rest, the membrane must resist a 1 bar (10^5 Pa) pressure difference. Under actuation it must break when a maximum constraint is reached. Because Si_3N_4 is brittle, the rupture threshold is obtained when the first maximum constraint is larger than the constraint

$$\sigma_{\max} = \alpha\ E/(2(1+\nu)) \quad (10)$$

where E and ν are the Young modulus and Poisson ratio, and α a coefficient of the order of 1/20. For silicon nitride, relation (10) indicates an approximate value of 2-3 10^9 Pa.
The calculation of the membrane deformation and stress is based on the relation between the stress tensor Σ and the forces F

$$-\nabla.\Sigma = F \quad (11)$$

taking into account the stress-strain relationship $\Sigma = D\varepsilon$ where D is the elasticity matrix. Membrane deformation is calculated by using the COMSOL numerical software. As expected, the location of the maximum of the constraints is at the contact between the electrode and the membrane (fig. 6 and 7).

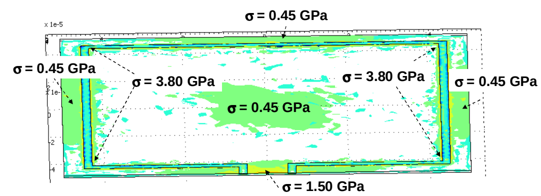

Fig.6. Density of deformation energy [Pa] is concentrated along the grooves.

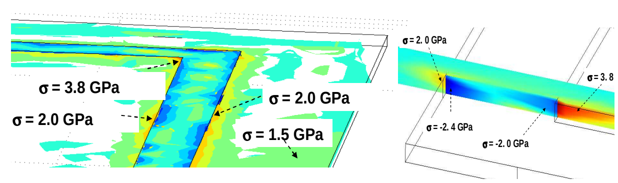

Fig.7. Constraints are maximum along the electrode vertical walls at the contact with the Si_3N_4, particularly in the corners.

The calculation shows that a maximum temperature of 1100 K, obtained with a 3 Volts peak electric potential is sufficient to obtain a maximum stress of 3.8 10^9 Pa and cause the failure of the membrane.

5 DETERMINATION OF THE BREAKUP THRESHOLD

A preliminary series of experiments have been performed with plain (no electrode) membranes in order to determine the breaking stress of Si_3N_4 membranes. The pressure on the membrane was progressively increased until breakup. Different sizes of 200nm-thick square membranes have been tested. Each time, the pressures have been measured by a microsensor and recorded, leading to the relation $P_{BU} = f(L)$, where P_{BU} is the pressure at breakup and L the dimension of the membrane. Breakup pressure as a function of the side dimension is shown in figure 8. The points reported in the figure are averaged on 10 to 15 experimental records. The breakup pressure decreases with an increase of the membrane surface area.

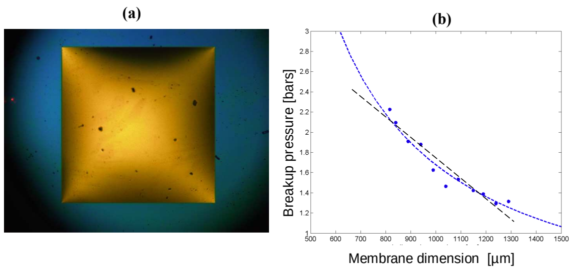

Fig.8. (a) View of a membrane deformed by the applied pressure; (b) breakup pressure versus side dimension of the membrane, showing the experimental data and the linear and hyperbolic fits.

On the other hand, the calculation has shown that the maximum stress in the membrane is a function of the membrane dimension L and the applied pressure P. This function can be symbolized by $\sigma_{\max} = g(P, L)$. We can then find the ultimate stress

$$\sigma_{BU} = g(P_{BU}, L) = g(f(L), L) = G(L) \qquad (12)$$

showing that the ultimate stress is a function of L. The values of the ultimate stress as a function of the membrane dimension are plotted in figure 9. The figure shows that very small membranes will have an ultimate stress of the order of 3 GPa.

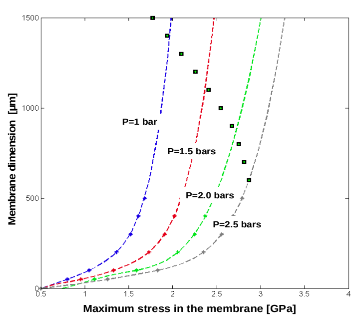

Fig.9. Maximum stress as a function of membrane dimension and applied pressure. The dots correspond to the ultimate stress.

6 CONCLUSION

We have numerically shown that thin membranes (200 nm) can be used as sacrificial membranes for valving in microfluidic systems when electrodes of the proper size are embedded in the membrane. These membranes can withstand a pressure larger than 1 bar without breaking. Upon actuation of a gold electrode under a potential of approximately 3 Volts, the dilatation of the electrode exerts a stress sufficient to obtain membrane breakup.

The results of the modeling have led to the design of sacrificial membranes. Experimental testing on these membranes is now underway to assess the numerical conclusions, and to investigate further the breakup morphology, i.e. if the membrane breaks into small pieces or in a unique, large aperture.

REFERENCES

[1] H. Cho, H-Y Kim, J.Y. Kang and T.S. Kim, “Capillary Passive Valve in Microfluidic System,” Technical Proceedings of the 2004 NSTI Nanotechnology Conference and Trade Show, Volume 1, 2004

[2] Yoon-Kyoung Cho, Jeong-Gun Lee, Jong-Myeon Park, Beom-Seok Lee, Youngsun Lee and Christopher Ko, “One step pathogen specific DNA extraction from whole blood on a centrifugal microfluidic device,” Technical Proceedings of the 2007 NSTI Nanotechnology Conference and Trade Show, 2007

[3] M. Koch, A. Evans, A. Brunnschweiler. Microfluidic Technology and Applications. Research Studies Press LTD, 2000

[4] V. Studer, Giao Hang, A. Pandolfi, M. Ortiz, W. F. Anderson, S. R. Quake, “Scaling properties of a low-actuation pressure microfluidic valve,” J. Applied Physics, Vol. 95, n°1, pp. 393-399, 2004

[5] H. Esfandyarpour, R.W. Davis, “Microfluidic Valve-Controllable Magnetic Bead Receptacle: A Novel Platform for DNA Sequencing,” Technical Proceedings of the 2007 NSTI Nanotech Conference, Vol. 3, 2007

[6] K.W. Ohl, C.H. Ahn, “A review of microvalves,” J. Micromech. Microeng., Vol.16, pp. R13–R39, 2006

[7] M. L Cardenas, A. M. Cardenas-Valencia, J. Dlutowski, J. Bumgarner and L. Langebrake, “A finite element method modeling approach for the development of metal/silicon nitride MEMS single-use valve arrays,” J. Micromech. Microeng., Vol. 17; pp. 1671–1679, 2007

[8] R.E. Cavicchi, C.T. Avedisian, “Bubble Nucleation and Growth Anomaly for a Hydrophilic Microheater Attributed to Metastable Nanobubbles,” Physical Review Letters, Vol. 98, p. 124501, 2007

[9] O. Thomas, R.E. Cavicchi, M.J. Tarlov, “The effect of surface wettability on fast transient microboiling behavior,” Langmuir, to be published.

[10] J. Buongiorno, “Boiling behavior of nanofluids,” Course at the CISM, 1-5 September 2008, Udine, Italy